THE JOURNAL OF COMPARATIVE NEUROLOGY 485:1–10 (2005)

Redefining the Boundaries of the Hippocampal CA2 Subfield in the Mouse Using Gene Expression and 3-Dimensional Reconstruction

EDWARD S. LEIN,[1–3] EDWARD M. CALLAWAY,[2] THOMAS D. ALBRIGHT,[3,4] AND FRED H. GAGE[1]*

[1]Laboratory of Genetics, The Salk Institute for Biological Studies, La Jolla, California 92037
[2]Systems Neurobiology Laboratory, The Salk Institute for Biological Studies, La Jolla, California 92037
[3]Vision Center Laboratory, The Salk Institute for Biological Studies, La Jolla, California 92037
[4]Howard Hughes Medical Institute, State University of New York at Stony Brook, Stony Brook, New York 11794

ABSTRACT

The morphology of neurons in the main divisions of the hippocampal complex allow the easy identification of granule cells in the dentate gyrus and pyramidal cells in the CA1 and CA3 regions of Ammon's horn. However, neurons in the CA2 subfield have been much more difficult to reliably identify. We have recently identified a set of genes whose expression is restricted to either the dentate gyrus, CA1, CA2, or CA3. Here we show that these genes have an essentially nonoverlapping distribution throughout the entire septotemporal extent of the hippocampus. 3-Dimensional reconstruction of serial sections processed for in situ hybridization of mannosidase 1, alpha (CA1), bcl-2-related ovarian killer protein (CA3), and Purkinje cell protein 4 (dentate gyrus + CA2) was used to define the boundaries of each subregion throughout the entire hippocampus. The boundaries observed for these three genes are recapitulated across a much larger set of genes similarly enriched in specific hippocampal subregions. The extent of CA2 defined on the basis of gene expression is somewhat larger than that previously described on the basis of structural anatomical criteria, particularly at the rostral pole of the hippocampus. These results indicate that, at least at the molecular level, there are robust, consistent genetic boundaries between hippocampal subregions CA1, CA2, CA3, and the dentate gyrus, allowing a redefinition of their boundaries in order to facilitate functional studies of different neuronal subtypes in the hippocampus. J. Comp. Neurol. 485:1–10, 2005. © 2005 Wiley-Liss, Inc.

Indexing terms: CA1; CA2; CA3; dentate gyrus; in situ hybridization; fasciola cinerea

The fine structure of the hippocampal formation has been extensively studied for over a century using a wide variety of techniques (Claiborne et al., 1986; Lorente de Nó, 1934; Ramón y Cajal, 1911; Swanson et al., 1981). Nissl and Golgi staining demonstrate clear divisions between granule cells of the dentate gyrus and pyramidal cells of Ammon's horn, which consists of a regio superior containing small pyramidal neurons and a regio inferior containing large pyramidal neurons (Golgi, 1886; Lorente de Nó, 1934; Ramón y Cajal, 1911). On the basis of Golgi impregnation of hippocampal neurons, Lorente de Nó further defined regions within Ammon's horn, with CA1 corresponding to regio superior, CA3 to most of regio inferior, and CA2 to a small boundary zone between CA1 and CA3 that does not receive mossy fiber input from the dentate gyrus, and which lacks the specialized postsynaptic"thorny excrescences" characteristic of mossy fiber synapses (Bartesaghi and

Grant sponsor: National Institute on Aging; Grant number: AG06088; Grant sponsor: The Christopher Reeves Paralysis Foundation; Grant sponsor: David and Lucile Packard Foundation; Grant sponsor: National Institutes of Health Bioengineering Research Partnership; Grant number: EY14103.

Dr. Lein's present address is Allen Institute for Brain Science, 551 N. 34th Street, Seattle, WA 98103. E-mail: edl@alleninstitute.org

*Correspondence to: Fred H. Gage, Laboratory of Genetics, The Salk Institute for Biological Studies, 10010 N. Torrey Pines Road, La Jolla, CA 92037. E-mail: gage@salk.edu

Received 15 April 2004; Revised 20 July 2004; Accepted 7 September 2004

DOI 10.1002/cne.20426

Published online in Wiley InterScience (www.interscience.wiley.com).

© 2005 WILEY-LISS, INC.

Ravasi, 1999; Ishizuka et al., 1995; Lorente de Nó, 1934; Tamamaki et al., 1988).

Functional differences between these regions have been described by many other anatomical and physiological techniques. However, CA2 has remained somewhat of an anomaly, sometimes considered a separate region and sometimes simply as an intermingling of cells from CA1 and CA3 (Grove and Tole, 1999; Woodhams et al., 1993). Mounting evidence suggests that CA2 is an anatomically and functionally distinct region, although the boundaries of this region are unclear. One of the most compelling arguments for the existence of a discrete CA2 region comes from the growing number of molecules expressed specifically in the distal portion of regio inferior corresponding roughly to Lorente de Nó's CA2, or that are excluded from this region (Lein et al., 2004; Leranth and Ribak, 1991; Ochiishi et al., 1999; Sloviter et al., 1991; Tochitani et al., 2003; Tucker et al., 1993; Vigers et al., 2000; Williams et al., 1996). For example, fibroblast growth factor 2 (Fgf2) (Williams et al., 1996), adenosine A1 receptor (Ochiishi et al., 1999), and epidermal growth factor receptor (Egfr) (Tucker et al., 1993) are specifically expressed in CA2, while neurotrophin-3 (Ntf3) (Vigers et al., 2000) and Purkinje cell protein 4 (Zhao et al., 2001) are robustly expressed in the dentate gyrus and CA2 with no expression in CA1 and CA3. These markers define a remarkably distinct CA2 region, indicating that at least at the molecular level, CA2 is a discrete hippocampal subregion. However, the use of molecular markers to define CA2 has sometimes been problematic. For example, Fgf2, Ntf3, and Egfr are expressed in a more widespread fashion at the septal pole of the hippocampus than in more caudal planes of section, leading to descriptions of this rostral pattern of expression alternatively as an extension of CA2, as dorsal CA3, or as dorsal CA1 (Tucker et al., 1993; Vigers et al., 2000; Williams et al., 1996). It remains to be demonstrated whether this septal hippocampal region is indeed part of CA2 or rather the rostral extension of one of the other pyramidal zones.

A number of molecules defining each hippocampal subregion have been described (Lein et al., 2004). Neurons in CA1 are heavily enriched for nephroblastoma overexpressed gene (Nov) (Zhao et al., 2001), Tyro3 (Lai et al., 1994), SCIP (Frantz et al., 1994; Grove and Tole, 1999), and mannosidase 1, alpha (Man1a) (Lein et al., 2004). Neurons in CA3 are enriched for protein kinase C delta (Prkcd) (Zhao et al., 2001) and bcl-2-related ovarian killer protein (Bok) (Lein et al., 2004). Finally, dentate gyrus granule cells uniquely express desmoplakin (Lein et al., 2004) and insulin-like growth factor binding protein (Zhao et al., 2001). Genes displaying such highly restricted patterns of expression provide powerful tools for the examination of anatomical boundaries within complex brain structures, with the assumption that consistent molecular boundaries define functionally distinct brain regions.

We previously identified a large series of genes with restricted patterns of expression in one or more hippocampal subfield (Lein et al., 2004; Zhao et al., 2001). In order to clarify the boundaries between these regions, in the present study we used a set of genes that define the different hippocampal subregions CA1, CA2, CA3, and the dentate gyrus to unambiguously define genetic boundaries of these regions throughout the entire septotemporal extent of the hippocampal formation, using in situ hybridization for subfield-specific genes on serial brain sections, and 3D reconstruction to examine simultaneously the full extent of each molecularly defined subfield.

MATERIALS AND METHODS

Animals and tissue

All animal procedures were performed according to protocols approved by The Salk Institute for Biological Studies Animal Care and Use Committee. C57BL/6 10–11-week-old male mice were obtained from Harlan (San Diego, CA). Mice were euthanized by intraperitoneal injection of a mixture of ketamine (75 mg/kg), xylazine (4 mg/kg) and acepromazine (5.6 mg/kg). For in situ hybridization, brains were rapidly dissected, rinsed in ice-cold 0.1 M phosphate buffer, frozen in OCT mounting medium (TissueTek; Sakura Finetek, Torrance, CA) in a dry ice-isopentane slurry, and stored at −80°C until use.

In situ hybridization

Clones for the genes analyzed were either ordered from the I.M.A.G.E. Consortium (Incyte Genomics, Palo Alto, CA) or amplified by PCR from mouse brain cDNA and cloned into the pCRII-TOPO cloning vector (Invitrogen, Carlsbad, CA). Sequence-confirmed plasmids were linearized and used for the synthesis of sense and antisense α-^{35}S-labeled riboprobes using T3, T7 (Stratagene, La Jolla, CA), or Sp6 (Promega, Madison, WI) RNA polymerases. Nomenclature from Mouse Genome Informatics (http://www.informatics.jax.org/) (Blake et al., 2003) was used to identify genes specifically analyzed in the current study as well as those cited in the literature. IMAGE clone identifiers and PCR primers used to generate the clones used in this study are as follows. Mannosidase 1, alpha (Man1a): F 5′-ACAgATCTCgAAgCCAAgAAgA; R 5′-ACATgTATgTCTCgATgACCTC; Bcl-2-related ovarian killer protein (Bok): IMAGE clone 949789 (GenBank accession AA178190); Purkinje cell protein 4 (Pcp4): F 5′-AgTCAggCCAACATgAgTgAgA; R 5′-ACCACTAggACTgTgATCCTg.

In situ hybridization was performed as described previously (Lein et al., 2004), utilizing methodology to allow the processing of large numbers (~150) of slides simultaneously. Twelve micrometer coronal cryostat sections through the entire hippocampal formation were cut and mounted on Superfrost slides (Sigma, St. Louis, MO) in such a way that slide 1 contained section 1, 101, and 201, slide 2 contained section 2, 102, and 202, and so on. For 3D reconstruction, each probe in the series was hybridized to every fourth slide (e.g., slides 1, 5, 9), such that equal representation of in situ hybridization data was obtained for each probe (Man1a for CA1, Bok for CA3, and Pcp4 for the dentate gyrus and CA2) throughout the entire septotemporal extent of the hippocampus. The fourth section was stained using cresyl violet to allow a comparison of in situ hybridization labeling to Nissl staining at each plane of section. Processing in this way allowed a very detailed analysis of gene expression throughout the entire hippocampal formation. Sense controls in all cases yielded nonspecific background labeling (data not shown). Furthermore, all slides for a given probe were processed in parallel to allow comparisons of hybridization intensity throughout the entire hippocampus.

Following in situ hybridization, slides were first exposed to X-ray film (X-OMAT AR; Eastman Kodak, Rochester,

NY), subsequently defatted, and dipped in autoradiographic emulsion (NTB2; Eastman Kodak), and allowed to expose for $1\frac{1}{2}$–3 weeks depending on the strength of labeling observed on X-ray film. Slides were then developed and stained with the fluorescent dye bisbenzimide (Sigma, St. Louis, MO) to allow localization of silver grains to individual cells and to aid in the alignment process described below. Slides of in situ hybridization were digitized using a cooled CCD camera (SPOT2; Diagnostic Instruments, Sterling Heights, MI) mounted on a Nikon Eclipse TE300 microscope (Nikon, Melville, NY) using an external darkfield adapter (Darklite Vertical; Micro Video Instruments, Avon, MA). Contrast levels were adjusted using Adobe PhotoShop (Adobe Systems, San Jose, CA). Images from all sections for a given probe were generated using identical methodology (exposure settings and contrast adjustments) to allow a comparison of hybridization intensity across sections.

3D Reconstruction

Low-magnification (2×) images of each slide were obtained using darkfield illumination for the in situ hybridization signal and fluorescence for the bisbenzimide labeling. Adobe PhotoShop was then used to manually align the fluorescent (or Nissl-stained) images of serial sections, which were in turn used to put the darkfield images in register. Alignment was performed on a single hemisphere, using the midline as a fiducial point for alignment in the medial/lateral dimension, and the overall architecture of the entire brain in the dorsal/ventral dimension. In order to facilitate visualization of the reconstructed hippocampus, all images were digitally mirrored across the midline to produce a representation of both hemispheres. For each set of three serial aligned images, the grayscale in situ hybridization signal for each gene was inserted into a separate channel of an RGB file, thereby creating a false-colored montage of gene expression at that plane of section. At certain planes of section where the curvature of the hippocampus is extreme, for example, the caudal bend of the hippocampus, this overlaying led to a small amount of apparent overlap of different regions. However, at most planes of section the labeling of different hippocampal subfields appeared to be almost completely nonoverlapping. The hippocampus was then digitally "dissected" from surrounding brain regions to allow visualization of the hippocampus specifically. Artifacts from the autoradiographic process were also removed from the images at this point. A total of 65 photomontages representing all planes of section through the hippocampus were then assembled into a full 3D reconstruction using the 3D Constructor plug-in of Image-Pro Plus (v. 5.0; Media Cybernetics, Silver Spring, MD). In order to maintain an accurate 3D representation in the z (rostral/caudal) dimension, each individual photomontage was given the depth of four sections (48 μm, the sum of 12 μm sections for each gene in the photomontage plus 12 μm for the adjacent Nissl-stained section). The total depth in the rostral/caudal plane was therefore 65*48 μm = 3,120 μm, which is consistent with the rostral/caudal extent of the hippocampus described in available stereotaxic atlases of the adult C57Bl/6 mouse (Paxinos and Franklin, 2001). Surface renderings of each hippocampal subregion were also created using Image-Pro software. Since Pcp4 labels both the dentate gyrus and CA2, the in situ hybridization signal in CA2 was digitally dissected away from the noncontiguous dentate gyrus to allow the independent visualization of CA2.

RESULTS

Hippocampal subregions CA1, CA2, CA3, and the dentate gyrus can be differentiated on the basis of highly specific gene expression. In situ hybridization on serial thin cryostat sections demonstrates that expression of genes specific for each hippocampal subregion is nonoverlapping at dorsal planes of section through the hippocampus. For example, pyramidal neurons in CA1 express high levels of Man1a (Fig. 1B,G). Pyramidal neurons in CA3 are uniquely defined by expression of Bok (Fig. 1C,H), while dentate gyrus granule cells as well as pyramidal neurons in CA2 are defined by expression of Pcp4 (Fig. 1D,I). The boundaries of gene expression observed with these three genes perfectly match cytoarchitectural boundaries visible by cresyl violet staining (Fig. 1E,J), with the exception of the CA2/CA3 boundary, which is not visible using standard histological methods. On tissue processed for in situ hybridization, the boundary between CA1 and CA2 is very clearly delineated by staining with the fluorescent dye bisbenzimide (Fig. 1A,F), which provides a useful marker at planes of section in which this boundary is difficult to discern by Nissl staining.

The expression of Man1a, Bok, and Pcp4 was examined on serial thin cryostat sections through the entire hippocampus (Fig. 2). As shown for seven coronal planes of section, expression of each of these genes within their respective subregions is robust throughout the hippocampus (Fig. 2B–D). Since the cryostat sections used were very thin (12 μm), three consecutive sections do not vary significantly in their plane of section, allowing an approximation of triple-labeling by aligning, overlaying, and false-coloring adjacent sections stained for different subregion-specific probes. As shown in Figure 2E, with Man1a in red (CA1), Bok in green (CA3), and Pcp4 in blue (dentate gyrus + CA2), these three genes demonstrate essentially nonoverlapping expression throughout the entire septotemporal axis of the hippocampus. Pseudocolored overlays were generated from serial sections through the entire hippocampal formation, and the hippocampus was then "digitally dissected" away from the rest of the brain to allow an examination of the hippocampus alone (Fig. 2F). Finally, these overlays were used to produce a 3D representation of the hippocampus, based on gene expression delimiting the different subregions (Fig. 2G). It should be noted that Man1a is also expressed in a band of cells in the subiculum that is clearly distinguishable from the tight cell layer of CA1 (see Fig. 2E, final two panels). To visualize CA1 alone, this subicular expression was removed. Similarly, Bok expression in the ventral subiculum (Fig. 2E, final three panels) was removed in order to visualize CA2 in the absence of the subiculum. Furthermore, the overall 3D structure of the hippocampus is easier to grasp when viewing both hemispheres. Since care was taken during the process of aligning sections to maintain the position of the midline, it was possible to mirror the representation made from a single hemisphere across the midline to produce an accurate bihemispheric 3D representation of the hippocampus (Fig. 3).

3D representations of the entire hippocampus and each subregion alone are shown in several orientations in Figure 3. For the purposes of visualization, CA2 was sepa-

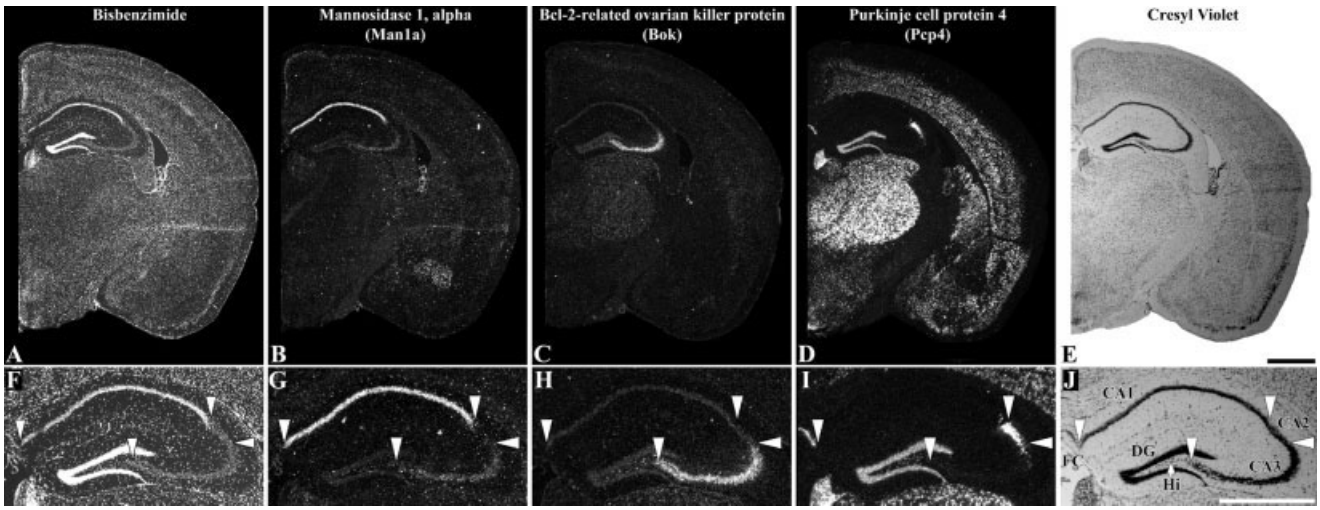

Fig. 1. Gene expression defines the boundaries of hippocampal subregions CA1, CA2, CA3, and the dentate gyrus. In situ hybridization for Man1a (**B,G**), Bok (**C,H**), and Pcp4 (**D,I**) on serial coronal sections through the dorsal hippocampus at low magnification (**B–D**) and high magnification (**G–I**). Cresyl violet staining is shown on an adjacent serial section (**E,J**), and bisbenzimide labeling of the same section in panels B and G is shown in panels **A** and **F**. Arrowheads in (F–J) delimit the boundaries of CA1, CA2, and CA3. Small arrow in J denotes the hilus of the dentate gyrus. CA1, CA2, CA3: pyramidal cells of the subdivisions of Ammon's horn; DG: dentate gyrus; Hi: hilus of the dentate gyrus; FC: fasciola cinerea. Scale bars = 1 mm.

rated and colored differently from the dentate gyrus, although the representation of these two structures was created from expression of the same gene. Visualized in three dimensions, each subfield of the hippocampus forms a coherent structure. The dentate gyrus forms a curving double-bladed structure that varies quite substantially along the septotemporal axis in the relative sizes of the dorsal and ventral blades, as well as the breadth of the space between the two blades. Furthermore, only the ventral blade of the dentate gyrus extends to the extreme dorsal and rostral (septal) pole, while the ventral (temporal) tip tapers dramatically and loses its double-bladed structure as it curves back anteriorly. Each subregion of Ammon's horn forms a coherent thin sheet of cells. CA3 is narrowest at the rostral (septal) end of the hippocampus and fans out somewhat at more ventral (caudal) levels. CA1, on the other hand, is broadest at rostral (septal) levels and tapers off at more ventral (caudal) levels. CA2, by contrast, forms a strip of remarkably uniform width throughout most of the hippocampus. Unexpectedly, at the extreme rostral (septal) tip of the hippocampus, CA2 wraps around CA1 and continues caudally down the midline (see Fig. 3C,G), as discussed below. The depth and curvature of each hippocampal subregion relative to the others is more easily appreciated in the stereo pairs shown in Figure 3E–H.

The boundaries of subfield CA2 demonstrated by 3D representation of gene expression differ somewhat from the boundaries defined in currently available stereotaxic mouse atlases (Hof et al., 2000; Paxinos and Franklin, 2001). These boundaries are examined in more detail on coronal sections through the septal pole of the hippocampus in Figure 4. At the very septal-most sections through the hippocampus, cresyl violet staining demonstrates that the dentate gyrus consists only of the infrapyramidal blade, and the pyramidal cell layer appears first as a patch of cells, which then opens up into a ring of cells (Fig. 4F). Nissl staining does not allow the accurate delineation of regio superior and regio inferior until ~500 μm into the hippocampus. The extreme septal pole of the pyramidal layer expresses only Bok (Fig. 4C), indicating that the pyramidal cells at this plane of section belong to subfield CA3. Beyond the very septal pole, however, the dorsal half of the expanding ring of pyramidal cells expresses Pcp4 to the exclusion of Bok (Fig. 4D), indicating that this region is in fact part of CA2, rather than CA3 as indicated by available stereotaxic atlases (for example, see fig. 40 of Paxinos and Franklin [2001] and p. 58 of Hof et al. [2000]). This dorsal portion of CA2 is split into two separate domains by the emergence of CA1, visualized by expression of Man1a (Fig. 4B), ~500 μm from the septal pole of the hippocampus. Interestingly, this most septal portion of CA1 cannot be easily distinguished on the basis of Nissl staining either, although it is apparent by bisbenzimide labeling (Fig. 4A, sixth panel). The more medial portion of CA2 continues caudally along the midline, becoming continuous with the fasciola cinerea (see Fig. 1I), as noted by other molecular studies of genes enriched in CA2 (Vigers et al., 2000). Although it is difficult to determine without true double labeling on the same sections, it appears that there is some mingling of cells expressing Bok and Pcp4 near the septal pole, and to a lesser extent at the CA2/CA3 boundary, indicating that, unlike the boundary between CA1 and CA2, the boundary between CA2 and CA3 is not exceptionally sharp.

DISCUSSION

The hippocampal CA2 field has been a difficult structure to define on the basis of anatomical criteria. CA2 was originally defined on the basis of Golgi impregnation as a small border region between CA1 and CA3 characterized by large pyramidal neurons that do not receive mossy fiber input from the dentate gyrus and lack the "thorny excres-

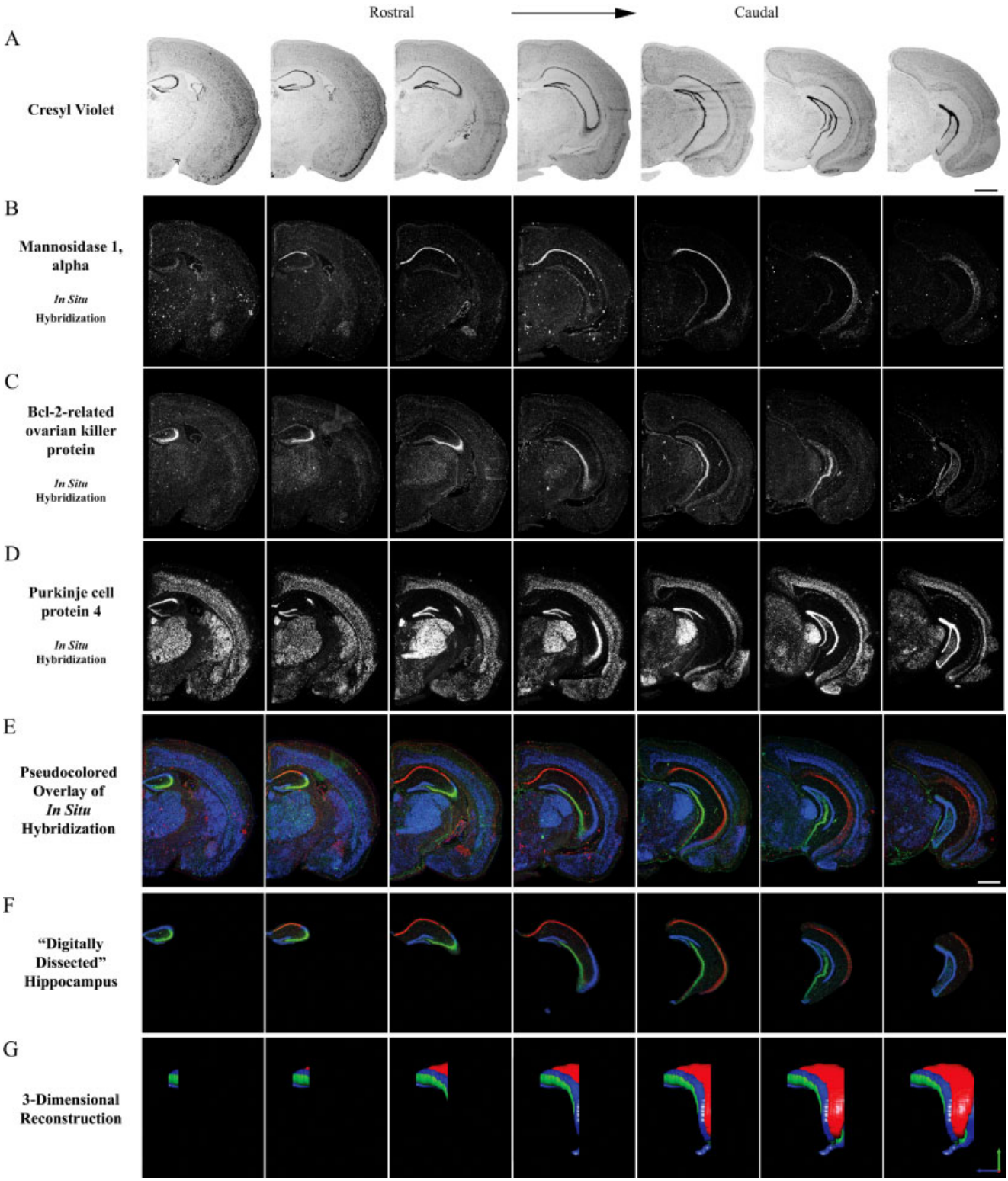

Fig. 2. Construction of a 3D representation of the hippocampus based on subregion-specific gene expression. **A:** Cresyl violet staining of coronal sections at seven planes of section spanning the rostral-caudal extent of the hippocampus. **B–D:** In situ hybridization for Man1a (B), Bok (C), and Pcp4 (D) on serial sections adjacent to those shown in (A). **E:** Pseudocolored overlays of aligned sections of in situ hybridization from panels B–D, with Man1a expression in CA1 in red, Bok expression in CA3 in green, and Pcp4 expression in the dentate gyrus and CA2 in blue. **F:** Pseudocolored overlays of gene expression in the hippocampus, "digitally dissected" away from the rest of the brain. **G:** Lateral view of the emerging 3D reconstruction of the hippocampus, from the rostral end of the hippocampus up to the corresponding panel in F. Orientation bars for 3D reconstruction: green arrow points to dorsal; blue arrow points to rostral; red arrow points from lateral to medial of the left hemisphere. Scale bar = 1 mm.

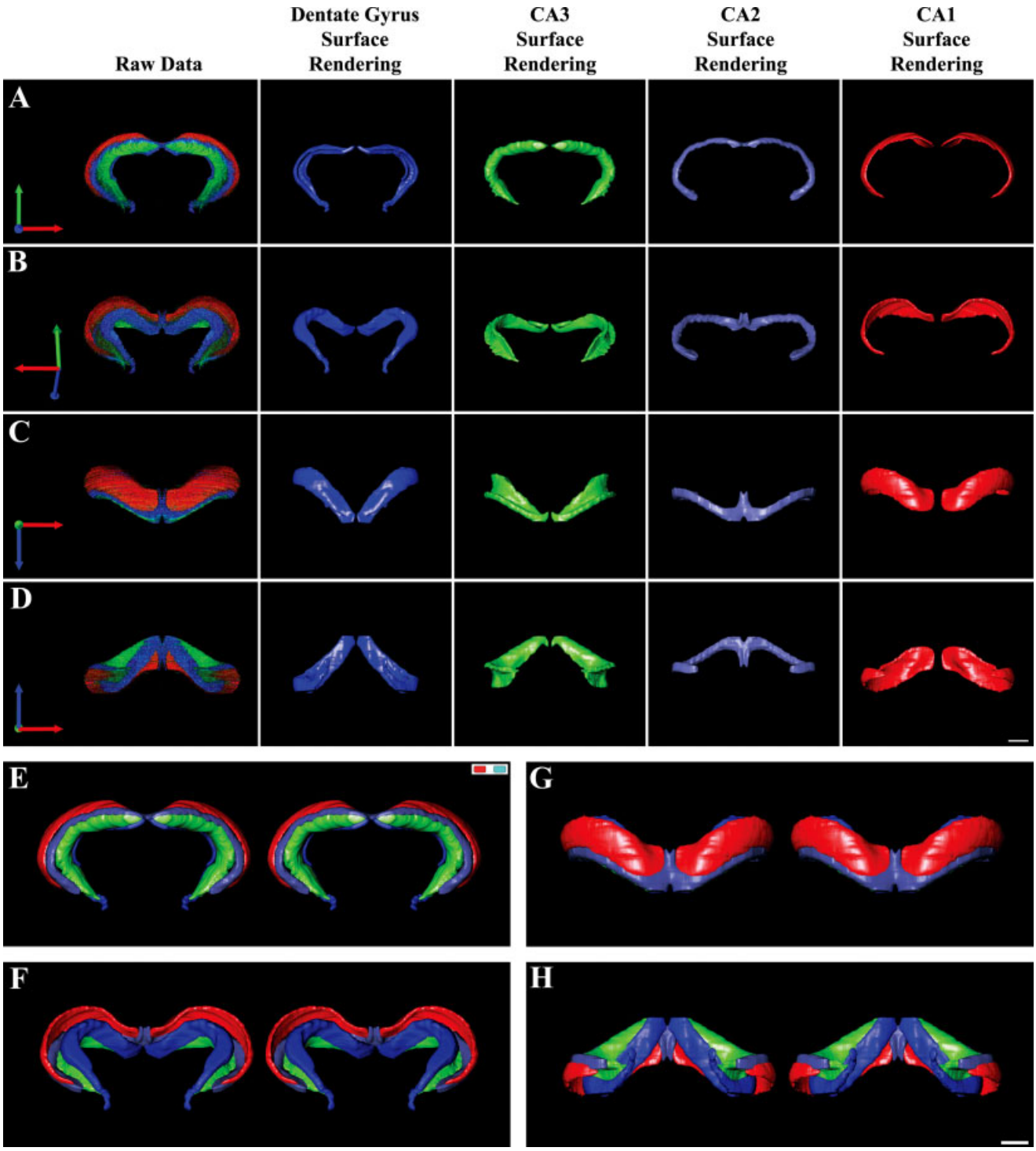

Fig. 3. 3D representation of the hippocampus based on gene expression. **A–D:** Four views of the entire hippocampus and each subregion alone at different orientations rotated around the medial/lateral axis. The raw data is shown in the left panel and surface renderings of each individual subregion are shown on the panels to the right. **E–H:** Stereo pairs of a combined representation of surface renderings for each hippocampal subregion, corresponding to panels A–D. Orientation bars for 3D reconstruction: green arrow points to dorsal; blue arrow points to rostral; red arrow points from lateral to medial of the left hemisphere. Scale bar = 1 mm.

cences" characteristic of CA3 pyramidal neurons (Lorente de Nó, 1934). Although this basic feature of CA2 neurons has been largely borne out by subsequent studies of single CA2 neurons (Bartesaghi and Ravasi, 1999; Ishizuka et al., 1995; Tamamaki et al., 1988), Timm's staining of granule cell mossy fibers does not end abruptly at the

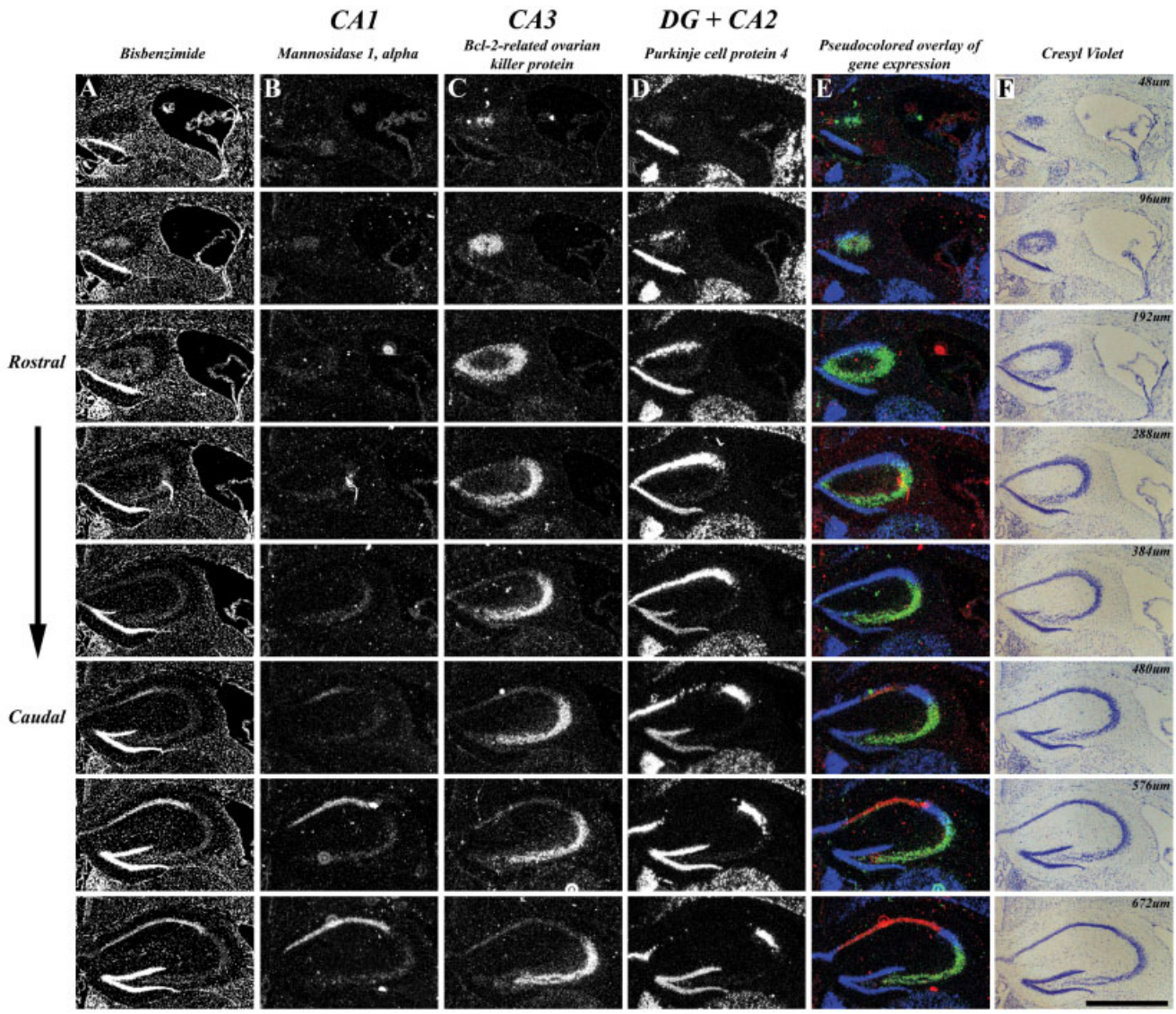

Fig. 4. Molecular boundaries of hippocampal subregions at the septal pole of the hippocampus. In situ hybridization for Man1a, Bok, and Pcp4 at eight planes of section on serial coronal sections through the rostralmost 700 μm of the hippocampus (**B–D**). **E:** Pseudocolored overlay of gene expression in panels B–D, demonstrating nearly non-overlapping expression of Man1a in CA1 (red), Bok in CA3 (green), and Pcp4 in the dentate gyrus and CA2 (blue). Cresyl violet staining of sections adjacent to those in panels B–D is shown in panel **F**, and bisbenzimide labeling of the same sections in panel B are shown in panel A. Micron measurements in panel F denote the distance of the Nissl-stained sections from the rostral pole of the hippocampus. Scale bar = 1 mm.

CA3/CA2 boundary, but rather tapers off towards the border of CA1 (Gaarskjaer, 1986), indicating that there is some mossy fiber input to the CA2 region. Furthermore, single neurons in CA2 share morphological characteristics with either CA1 or the proximal portion of CA3 (CA3a) (Bartesaghi and Ravasi, 1999; Ishizuka et al., 1995; Tamamaki et al., 1988), leading to some contention regarding the definition of CA2 as a distinct hippocampal subregion rather than a transition zone between CA3 and CA1 (Gaarskjaer, 1986; Woodhams et al., 1993).

Molecular markers provide powerful tools to assess functional boundaries between discrete brain regions. Consistent boundaries of gene expression presumably reflect divisions between functionally distinct neuronal types, regardless of the function of the particular genes. The advent of technologies to assess gene expression in discrete tissues on a genomic level, through the use of DNA microarrays, has produced a dramatic expansion in the availability of molecular markers with highly specific expression in discrete brain regions (Lein et al., 2004; Zirlinger et al., 2001). In the current study, a set of genes previously identified on the basis of heavily enriched expression within different hippocampal subregions (Lein et al., 2004; Zhao et al., 2001) was examined in much greater detail in order to clarify the boundaries between these regions. Consistent with previous studies (Lein et al., 2004; Tole et al., 1997) CA1, CA2, CA3, and the dentate gyrus each display a unique pattern of gene expression.

Processing of serial thin cryostat sections for genes enriched in different hippocampal regions and overlaying the expression patterns very closely approximates multiple-labeling on the same tissue section, and demonstrates that gene expression defining CA1, CA2, CA3, and the dentate gyrus is very nearly nonoverlapping throughout the entire septotemporal extent of the hippocampus.

In contrast to a situation in which CA2 consists of an intermingling of cells from CA1 and CA3, expression of Pcp4 defines a remarkably discrete CA2 region in the mouse. Similar observations have been made using a number of markers that define CA2 in the adult rodent, including Fgf2 (Williams et al., 1996), Ntf3 (Vigers et al., 2000), IGFBP4 (Stenvers et al., 1994), Trek2 (Gu et al., 2002), adenosine A1 receptor (Ochiishi et al., 1999), Egfr (Tucker et al., 1993), and Orc4l (unpubl. obs.). A much clearer picture of the overall structure and specificity of CA2 emerges when viewed in three dimensions. 3D reconstruction of gene expression for Pcp4 demonstrates that CA2 consists of a thin zone sandwiched between, but nonoverlapping with CA1 (as defined by Man1a) and CA3 (as defined by Bok), that is of fairly uniform width along almost the entire rostral-caudal extent of the hippocampus. Although such a reconstruction was only produced using the three genes described above, similar boundaries are recapitulated across a much larger set of genes with enriched expression in one or more hippocampal subregion (Lein et al., 2004; unpubl. obs.), indicating that there are consistent genetic boundaries that mirror cytoarchitectural boundaries within the hippocampus.

The robust, specific, and consistent boundaries of gene expression observed throughout the hippocampus allow a redefinition of boundaries in portions of the hippocampus where cytoarchitectural boundaries are unclear, such as the rostral (septal) pole of the hippocampus. Gene expression at the rostral pole defines a CA2 subfield that is somewhat more extensive than that described on the basis of anatomical criteria. Viewed in the coronal plane of section, CA2 comprises the entire dorsal half of the pyramidal layer at the rostral pole, and is split into a medial and lateral component by CA1 when it appears. Interestingly, although the emergence of CA1 at rostral planes of section cannot be distinguished on the basis of Nissl stains, the fluorescent dye bisbenzimide clearly labels the boundaries of CA1 throughout the hippocampus. Unlike currently available mouse (Hof et al., 2000; Paxinos and Franklin, 2001) and rat (Paxinos and Watson, 1998; Swanson, 2003) stereotaxic atlases, the rostral extension of CA1 ends fairly caudally, with CA2 forming what would otherwise be called regio superior for the most rostral 500 μm of the hippocampus. The lateral component of CA2 forms the boundary region between CA1 and CA3. The medial component, on the other hand, continues posteriorly and is continuous with the fasciola cinerea.

Similar rostral boundaries have been described several times in the literature. Previous studies examining genes with specific expression in CA2 have noted an expansion at the rostral pole of the hippocampus as well as a contiguous midline extension, leading to substantial confusion regarding nomenclature in the absence of simultaneous markers for the other hippocampal subregions. For example, Williams et al. (1996) noted two zones of Fgf2 expression that were continuous at the rostral end of the hippocampus, leading the authors to conclude that both zones were part of CA2. A study using a transgenic mouse expressing lacZ in the Ntf3 locus noted a similar pattern (Vigers et al., 2000), but referred to the most rostral portion as CA3. Expression of Igfbp4 (Stenvers et al., 1994) displays patterns similar to those described above, but the rostral expression was referred to as "the medial two-thirds of the CA1 pyramidal cell layer and the entire CA2 pyramidal cell layer," and dorsorostral expression of Egfr was similarly referred to as CA1 (Tucker et al., 1993, p. 95). It is clear that all of the known genes enriched in CA2 present the same pattern of expression in the rostral hippocampus, indicating that there is a clear genetically defined region including a small zone between CA1 and CA3, as well as the dorsal portion of the pyramidal cell layer in the rostral 500 μm of the hippocampus, and perhaps also the fasciola cinerea extending caudally along the midline. Interestingly, an identical pattern of hippocampal damage is observed following occlusion of the common carotid or posterior communicating arteries to the hippocampus (Akai and Yanagihara, 1993), encompassing CA2 and a contiguous population of neurons projecting down the midline (here referred to as "subiculum-CA1"), indicating that this zone is also functionally distinct, at least with respect to susceptibility to insults.

The availability of markers specific for the different subregions of the hippocampus allows an examination of the genetic relationship of neurons in the poorly understood fasciola cinerea with other types of pyramidal neurons. The fasciola cinerea in the mouse and rat refers to a small group of pyramidal neurons in the dorsal hippocampus that is discontinuous with the rest of Ammon's horn except at the extreme rostral pole. It should be noted that the term fasciola cinerea has not always been used to describe the same anatomical structure, and is sometimes used to describe the dorsocaudal extension of the dentate gyrus observed in some species such as the rabbit (see Hjorth-Simonsen and Zimmer, 1975, for a discussion of this subject). As described above, many genes with enriched expression in CA2 are also expressed in a continuous fashion with the fasciola cinerea, including Pcp4 (see Fig. 1), Ntf3 (Vigers et al., 2000), TREK1 (Gu et al., 2002), Egfr (Tucker et al., 1993), and Orc4l (unpubl. obs.). No expression in the fasciola cinerea was ever observed for genes whose expression is restricted to CA1, CA3, or the dentate gyrus alone (unpubl. obs.), indicating that at a genetic level the fasciola cinerea can perhaps be considered an extension of CA2. However, in some cases genes expressed in the entire regio inferior, encompassing both CA2 and CA3, are not expressed in the fasciola cinerea (unpubl. obs.). Therefore, a safer conclusion would be that neurons in the fasciola cinerea are most closely related to, but not identical to, neurons in CA2.

Taken together, it is clear that the CA1, CA2, and CA3 subdivisions of the hippocampus defined by Lorente de Nó (1934) each have a robust genetic counterpart. However, it remains to be shown that the molecularly defined CA2 region corresponds to Lorente de No's (1934) criteria of a region whose neurons do not receive mossy fiber input and lack corresponding "thorny excrescencies." There is in fact some discrepancy in the size of CA2 defined by these two sets of criteria. For example, based on anatomical criteria, Swanson et al. (1978) described a CA2 region ~100–150 μm in width in the rat. Other studies of individual CA2 neurons in the rat describe a CA2 between ~100 μm (Ishizuka et al., 1995) and 200 μm (Tamamaki et al., 1988), extrapolated from figures in these articles. By con-

trast, studies of gene expression in CA2 have defined a somewhat wider breadth. For example, Fgf2 immunoreactivity in the rat spans ~500 μm (Williams et al., 1996). Extrapolating from figures of other gene expression studies in the rat indicates a span of ~250 μm for adenosine A1 receptor (see fig. 2C of Ochiishi et al., 1999), and close to 500 μm for the EGF receptor (see fig. 3C of Tucker et al., 1993). Measurements across the short axis of CA2 from the current 3D representation based on Pcp4 expression in the mouse indicate a CA2 between 300 and 400 μm in width. Therefore, it would appear that the extent of CA2 defined molecularly is broader than that defined on the basis of Lorente de No's criteria of lack of mossy fiber input. An alternative anatomical correlate may be the termination zone of afferent projections. For example, the hypothalamic projection from the supramammilary nucleus terminates in a zone containing both CA2, as defined as the region lacking mossy fiber input, as well as the proximal portion of Lorente de No's CA3 (CA3a) (Stanfield and Cowan, 1984). Consistent with this idea, expression of the adenosine A1 receptor overlaps with labeling for mossy fibers in the stratum lucidum (Ochiishi et al., 1999), extending beyond the anatomically defined CA2 into CA3a.

It should be noted that anatomical observations of individual CA2 neurons indicate that there are multiple populations of neurons within CA2 that can be distinguished on the basis of dendritic morphology and axonal projections (Ishizuka et al., 1995; Tamamaki et al., 1988). Since there appears to be very little overlap of gene expression between the different subregions, this in turn suggests that multiple subtypes of CA2 neurons exist that are distinct from those of CA1 and CA3. Consistent with this idea, expression of Fgf2 protein is only observed in ~25% of the neurons in rat CA2 (Williams et al., 1996). Unfortunately, as it is not possible to distinguish the signal from individual neurons in densely packed structures on the basis of silver grain autoradiography, we cannot determine the proportion of labeled cells in the material used for the current study. True double-labeling with multiple CA2-specific markers will help to understand how many types of neurons exist in CA2. In addition, a tremendous benefit of genetic markers is that they open an avenue for the genetic manipulation of specific CA2 neuronal populations, by harnessing their promoters to drive the cell-type specific expression of transgenes. Genetic labeling and manipulation of CA2 neurons based on these markers should help to cross the gap between molecular neuroanatomy and structural neuroanatomy, as a means to ultimately understand the function of the elusive hippocampal CA2 field.

ACKNOWLEDGMENTS

We thank Tara Martinez and Becky Davis for expert technical assistance with in situ hybridization and image processing for 3D reconstruction. TDA is an investigator of the Howard Hughes Medical Institute.

LITERATURE CITED

Akai F, Yanagihara T. 1993. Identity of the dorsal hippocampal region most vulnerable to cerebral ischemia. Brain Res 603:87–95.

Bartesaghi R, Ravasi L. 1999. Pyramidal neuron types in field CA2 of the guinea pig. Brain Res Bull 50:263–273.

Blake JA, Richardson JE, Bult CJ, Kadin JA, Eppig JT. 2003. MGD: the Mouse Genome Database. Nucleic Acids Res 31:193–195.

Claiborne BJ, Amaral DG, Cowan WM. 1986. A light and electron microscopic analysis of the mossy fibers of the rat dentate gyrus. J Comp Neurol 246:435–458.

Frantz GD, Bohner AP, Akers RM, McConnell SK. 1994. Regulation of the POU domain gene SCIP during cerebral cortical development. J Neurosci 14:472–485.

Gaarskjaer FB. 1986. The organization and development of the hippocampal mossy fiber system. Brain Res 396:335–357.

Golgi C. 1886. Sulla Fina Anatomia Deglia Orani Centrali del Sistema Nervoso. Milano: U. Hoepli.

Grove EA, Tole S. 1999. Patterning events and specification signals in the developing hippocampus. Cereb Cortex 9:551–561.

Gu W, Schlichthorl G, Hirsch JR, Engels H, Karschin C, Karschin A, Derst C, Steinlein OK, Daut J. 2002. Expression pattern and functional characteristics of two novel splice variants of the two-pore-domain potassium channel TREK-2. J Physiol 539:657–668.

Hjorth-Simonsen A, Zimmer J. 1975. Crossed pathways from the entorhinal area to the fascia dentata. I. Normal in rabbits. J Comp Neurol 161:57–70.

Hof PR, Young WG, Bloom FE, Belichenko PV, Celio MR. 2000. Comparative cytoarchitectonic atlas of the C57BL/6 and 129/Sv mouse brains. Amsterdam: Elsevier.

Ishizuka N, Cowan WM, Amaral DG. 1995. A quantitative analysis of the dendritic organization of pyramidal cells in the rat hippocampus. J Comp Neurol 362:17–45.

Lai C, Gore M, Lemke G. 1994. Structure, expression, and activity of Tyro 3, a neural adhesion-related receptor tyrosine kinase. Oncogene 9:2567–2578.

Lein ES, Zhao X, Gage FH. 2004. Defining a molecular atlas of the hippocampus using DNA microarrays and high throughput in situ hybridization. J Neurosci 24:3879–3889.

Leranth C, Ribak CE. 1991. Calcium-binding proteins are concentrated in the CA2 field of the monkey hippocampus: a possible key to this region's resistance to epileptic damage. Exp Brain Res 85:129–136.

Lorente de Nó R. 1934. Studies on the structure of the cerebral cortex. II. Continuation of the study of the ammonic system. J Psychol Neurol (Lpz) 46:113–177.

Ochiishi T, Saitoh Y, Yukawa A, Saji M, Ren Y, Shirao T, Miyamoto H, Nakata H, Sekino Y. 1999. High level of adenosine A1 receptor-like immunoreactivity in the CA2/CA3a region of the adult rat hippocampus. Neuroscience 93:955–967.

Paxinos G, Franklin KBJ. 2001. The mouse brain in stereotaxic coordinates. San Diego: Academic Press.

Paxinos G, Watson C. 1998. The rat brain in stereotaxic coordinates. San Diego: Academic Press.

Ramón y Cajal S. 1911. Histologie du Système Nerveux. Maloine A, editor. Paris.

Sloviter RS, Sollas AL, Barbaro NM, Laxer KD. 1991. Calcium-binding protein (calbindin-D28K) and parvalbumin immunocytochemistry in the normal and epileptic human hippocampus. J Comp Neurol 308: 381–396.

Stanfield BB, Cowan WM. 1984. An EM autoradiographic study of the hypothalamo-hippocampal projection. Brain Res 309:299–307.

Stenvers KL, Zimmermann EM, Gallagher M, Lund PK. 1994. Expression of insulin-like growth factor binding protein-4 and -5 mRNAs in adult rat forebrain. J Comp Neurol 339:91–105.

Swanson LW. 2003. Brain maps III: structure of the rat brain. Burlington, MA: Academic Press/Elsevier.

Swanson LW, Wyss JM, Cowan WM. 1978. An autoradiographic study of the organization of intrahippocampal association pathways in the rat. J Comp Neurol 181:681–715.

Swanson LW, Sawchenko PE, Cowan WM. 1981. Evidence for collateral projections by neurons in Ammon's horn, the dentate gyrus, and the subiculum: a multiple retrograde labeling study in the rat. J Neurosci 1:548–559.

Tamamaki N, Abe K, Nojyo Y. 1988. Three-dimensional analysis of the whole axonal arbors originating from single CA2 pyramidal neurons in the rat hippocampus with the aid of a computer graphic technique. Brain Res 452:255–272.

Tochitani S, Hashikawa T, Yamamori T. 2003. Occ1 mRNA expression reveals a characteristic feature in the hippocampal CA2 field of adult macaques. Neurosci Lett 346:105–108.

Tole S, Christian C, Grove EA. 1997. Early specification and autonomous development of cortical fields in the mouse hippocampus. Development 124:4959–4970.

Tucker MS, Khan I, Fuchs-Young R, Price S, Steininger TL, Greene G, Wainer BH, Rosner MR. 1993. Localization of immunoreactive epidermal growth factor receptor in neonatal and adult rat hippocampus. Brain Res 631:65–71.

Vigers AJ, Baquet ZC, Jones KR. 2000. Expression of neurotrophin-3 in the mouse forebrain: insights from a targeted LacZ reporter. J Comp Neurol 416:398–415.

Williams TE, Meshul CK, Cherry NJ, Tiffany NM, Eckenstein FP, Woodward WR. 1996. Characterization and distribution of basic fibroblast growth factor-containing cells in the rat hippocampus. J Comp Neurol 370:147–158.

Woodhams PL, Celio MR, Ulfig N, Witter MP. 1993. Morphological and functional correlates of borders in the entorhinal cortex and hippocampus. Hippocampus 3 Spec No:303–311.

Zhao X, Lein ES, He A, Smith SC, Aston C, Gage FH. 2001. Transcriptional profiling reveals strict boundaries between hippocampal subregions. J Comp Neurol 441:187–196.

Zirlinger M, Kreiman G, Anderson DJ. 2001. Amygdala-enriched genes identified by microarray technology are restricted to specific amygdaloid subnuclei. Proc Natl Acad Sci U S A 98:5270–5275.